Vol. 201, No. 1, 1994 BIOCHEMICAL AND BIOPHYSICAL RESEARCH COMMUNICATIONS
May 30, 1994 Pages 346-355

FUR (FERRIC UPTAKE REGULATION) PROTEIN INTERACTION WITH TARGET DNA: COMPARISON OF GEL RETARDATION, FOOTPRINTING AND ELECTRON MICROSCOPY ANALYSES

Dominique Fréchon[1] and Eric Le Cam[2]*

[1] Laboratoire d'Ecologie Microbienne and [2] Laboratoire de Microscopie Cellulaire et Moléculaire, URA 147 du CNRS, Institut Gustave-Roussy, 94805 Villejuif Cedex, France

Received April 12, 1994

Fur-DNA interactions were analyzed within the regulatory regions of aerobactin and hemolysin operons by a combination of biochemical and ultrastructural methods. Cartography of the Fur binding sites, carried out from electron micrographs, agreed with the data obtained by DNase I footprinting. Visualization of the complexes confirmed the specificity and metal-dependence of Fur binding and demonstrated that the protein polymerizes on its binding sites. Such a polymerization could be involved in the repression process of the bacterial regulator.

© 1994 Academic Press, Inc.

The Fur (ferric uptake regulation) protein is a bacterial regulator which represses the expression of a number of iron acquisition genes and some other virulence determinants in *E. coli* (1). Fur uses ferrous iron (Fe^{2+}) as a corepressor and binds to a consensus sequence called "iron box", found in the promoter regions of various iron-regulated genes (2). The aerobactin operon, encoding a siderophore produced by numerous *Enterobacteriaceae*, has been used as a model for studying the regulation of gene expression by iron in *E. coli*. Two contiguous Fur-binding sites have been determined by DNase I footprinting in the major promoter (P1) of aerobactin operon (3). Another promoterlike sequences (P2) has been described upstream P1 but does not display an activity *in vivo* (4). In this system, as well as in several Fur-regulated systems (5-8), the presence of large footprints (30 to 50 bp) cannot be explained by the binding of two or even a few Fur molecules to target sites, with regard to the small size of the protein (17 kDa). To gain further insight into Fur binding processes within the regulatory region of the aerobactin operon, electron microscopy (EM) we used to get

*To whom correspondence should be addressed. Fax: (33 1) 47 26 92 74.

0006-291X/94 $5.00
Copyright © 1994 by Academic Press, Inc.
All rights of reproduction in any form reserved.

complementary information through the visualization and analysis of individual DNA-protein complexes (9).

Additional observations were obtained by using a hemolytic (*hly*) plasmid isolated from a human fecal *E. coli* strain, found to encode an iron-regulated hemolysin under control of the *fur* gene (10-12). In the *hly* determinant, we identified three specific sites upstream a major transcription initiation site. The results obtained by EM were compared with gel retardation and DNase I footprinting.

MATERIAL AND METHODS

Electron microscopy

The 645-bp *Hind*III-*Sal*I DNA fragment containing the aerobactin promoter, was obtained by digestion of the plasmid pABN5 (4) and Geneclean (BIO 101, USA) extraction. The hemolysin fragments A (370 bp) and B (270 bp) were synthesized by PCR (Fig. 1) and cloned respectively into the *Eco*RI and *Bam*HI sites of the vector pTZ19U (United States Biochemicals). Both fragments were recovered by double digestion and purified by elution from a 5 % polyacrylamide gel. The 1-kb *hly* *Sph*I-*Bam*HI fragment (Fig. 1) was obtained by digestion of the *hly* plasmid pANN681 (12) and Geneclean purification.

DNA templates and purified Fur protein (kindly provided by J. B. Neilands) were incubated in binding buffer (10 mM Tris pH 7.0, 40 mM KCl, 1 mM $MgCl_2$, 100 µM $MnCl_2$) at 37°C for 10 min. The complexes reported in this work result from protein/DNA ratio of 20 to 80 for aerobactin and 80 for hemolysin. DNA-protein complexes were purified by gel filtration on a Superose 6B micro-column with a chromatography SMART system (Pharmacia), and observed without addition of glutaraldehyde. The DNA fragments were not orientated since the ferritin used to orientate molecules (13) perturbs the visualization of the complexes obtained with short DNA fragments. Aliquots of 5 µl (DNA concentration 0.5 µg/ml) were deposited on carbon-coated grids, activated by glow-discharge in the presence of pentylamine (14). Specimens were contrasted with 2% aqueous uranyl acetate, dried and observed in annular dark-field using a Zeiss EM-902.

Fur-DNA complexes were observed at a final magnification of x340,000 on a TV screen. Images of Fur-bound DNA molecules were stored and digitized with a Kontron image processing system, as described previously (9,15). The data were processed in a PC computer and the DNA-protein interactions were mapped from 200 complexes. A computer test, which consisted in aligning the protections mapped by EM with those determined by footprinting, was used in order to discriminate the two Fur-binding sites contained in the non-orientated DNA fragments A. Two types of histograms were used, a classical one (type I) established from the centers of the interactions and another one (type II) taking into account the polymerization of Fur. To obtain the latter, the lengths of the DNA fragments were divided into 10-bp windows and all the protections identified in each window were reported into percentages of the total number of complexed molecules. Such a representation is more accurate for comparison with the footprinting methodology.

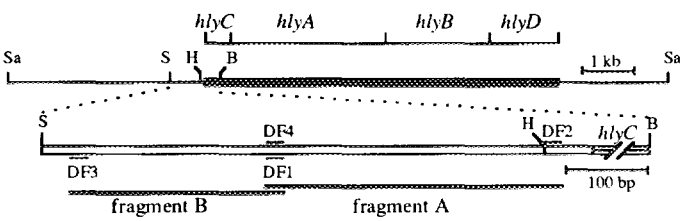

Fig. 1. **Schematic representation of the 5' non-coding DNA region of the hemolytic plasmid pANN681**. The recombinant plasmid pANN681 contains the 13.2-kb *hly* determinant from pGL681, cloned into the *Sal*I site of pACYC184 (7). Fragments A and B, generated by PCR using the primers DF1/DF2 and DF3/DF4 respectively, are represented by a dashed line. Restriction sites are indicated: B, *Bam*HI; H, *Hind*III; Sa, *Sal*I; S, *Sph*I.

Gel retardation assays and footprinting experiments

The aerobactin fragment was obtained as described above and labeled by fill-in with α-[^{32}P]dCTP and Klenow enzyme. The hemolysin fragments A and B were end-labeled by PCR. For each fragment, one of the two oligonucleotides was labeled with [γ-^{32}P]ATP and T4 polynucleotide kinase, prior to amplification. Incubation conditions were identical to those used for EM. The resulting duplexes were purified on a Sephadex G50 column. Gel retardation assays were performed as described (16), except that gels were run at pH 7.0. DNase I protection experiments were performed as described (3).

RESULTS

Analysis of Fur-DNA interactions by electron microscopy

Visualization of Fur-DNA complexes was unexpected with regard to the small size of the protein (17 kDa), thus indicating its oligomerization on the DNA (Figs. 2 and 3). Because observation of the complexes before or after chromatography did not show any difference, complexes were purified for a better visualization. Fur was found to bind target DNAs in a specific and metal-dependent manner, since no binding occured with pTZ19U vector DNA, as well as no complex was observed in the absence of metal ($MnCl_2$) or in the presence of the chelator 2,2'-dipyridyl.

Visualization and analysis of the complexes were performed with the aerobactin promoter, a well studied model for Fur-DNA interaction. A quantitative analysis of EM pictures provided Fur-DNA interaction maps (Fig. 2, H_a and H_b), as described in Material and Methods. Protections of 34 bp and 59 bp (Table I) obtained at molar ratios of 20 and 50 respectively, correspond to the protection of two sequentially occupied adjacent sites, as described by de Lorenzo *et al.* (3). At higher protein/DNA ratios (80 and 150), Fur polymerization extends beyond its recognition site. Interestingly, the major difference between the results obtained in both conditions lies in the percentage of bound molecules (78% and 96%) rather than in the size of DNA covered with Fur (83 bp and 89 bp). At a ratio of 150, a few molecules (2%) were totally covered and were not considered for mapping. At ratios of 50 and 80, as reported in Figs. 2a and 2b respectively, the distributions of the interaction centers (type I) display similar profiles, whereas those taking into account all the interactions (type II) illustrate the extension of the protection and the tendency of Fur to polymerize onto DNA. Furthermore, the asymmetry of the distribution at a ratio of 80 shows that Fur polymerization elongates in the 5' direction.

Initial EM observations were made with the *hly* *Sph*I-*Bam*HI (1-kb) fragment and revealed the binding of Fur within the regulatory region of hemolysin (not shown). In order to compare these results with gel retardation and footprinting experiments, two shorter fragments A and B were used (Fig. 1). Single and double-liganded complexes were visualized with the *hly* fragments A (Fig. 3 b_1, b_2), while single complexes only were observed with *hly* fragments B (Fig. 3 a). At a protein/DNA molar ratio of 80, 50% and 28% of the fragments A and B respectively were complexed with Fur, when a value of 78% was obtained with aerobactin molecules (Table 1), which indicates a better affinity of Fur for the aerobactin promoter. The average protections obtained for site I (41 bp) and site II (45 bp) contained in the fragment A agree with the footprints previously published for various Fur-regulated genes

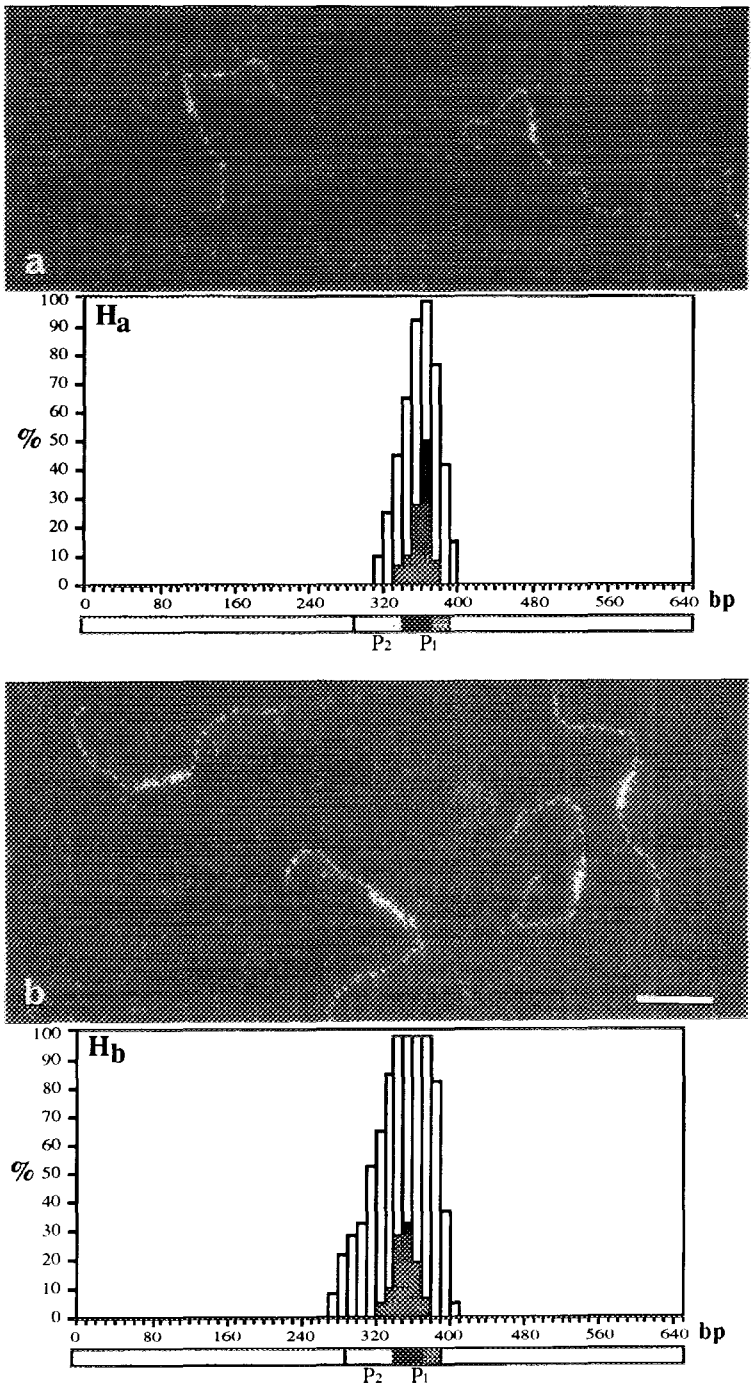

Fig. 2. **Electron micrographs and cartography of Fur-DNA complexes with the regulatory region of the aerobactin operon.** (**a**, **b**). Complexes obtained at a molar protein/DNA ratio of 50 and 80, respectively with a DNA fragment of 640 bp. The bar equals 50 nm.

Histogram with dark bars was established from the centers of interactions and reported in percentages of bound molecules. Histogram with light bars was obtained by reporting the total number of interactions (in %) within 10-bp windows, as described in Material and Methods. The three successive binding-sites determined by footprinting (black and grey segments for promoter P1, and white for P2) have been presented at the bottom of the graph.

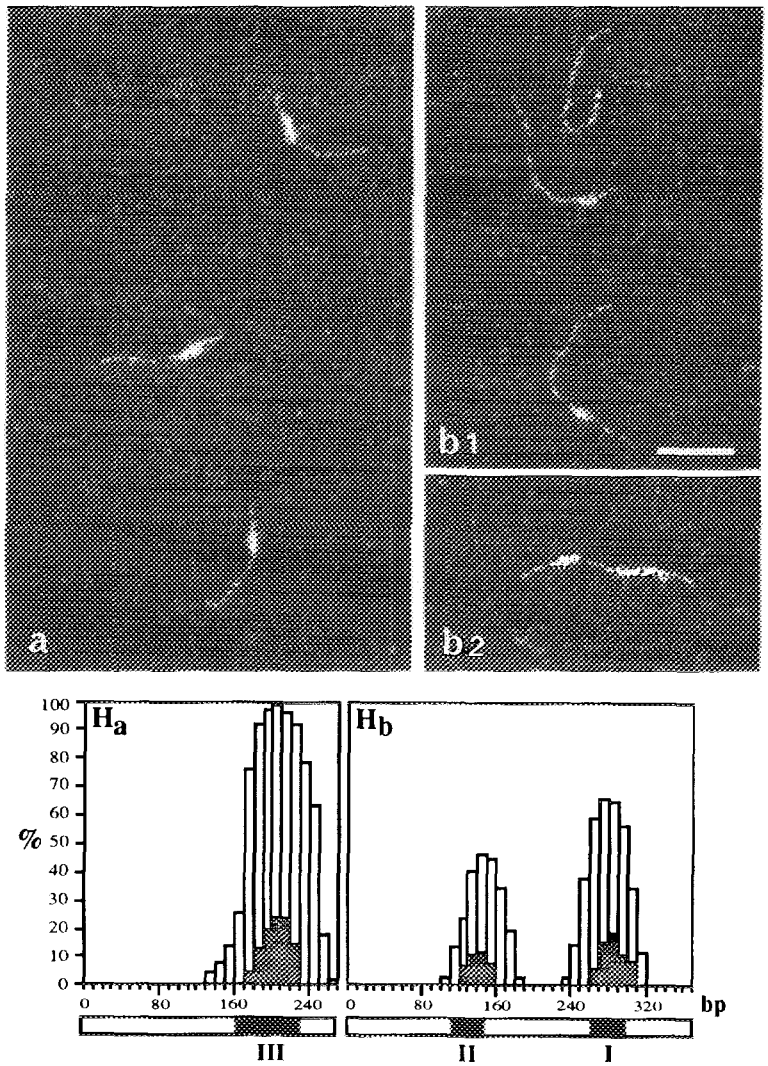

Fig. 3. **Electron micrographs and cartography of Fur-DNA complexes with the regulatory region of the hemolysin operon.** (**a**). Complexes with hemolysin B fragments (270 bp) containing the site III. (**b1**, **b2**). Single- and double-liganded complexes with hemolysin A fragments (370 bp) containing the sites I and II. All the hemolysin complexes have been obtained at a molar protein/DNA ratio of 80. The bar equals 50 nm.
The histograms were obtained as described in Fig. 2.

(3-8). In the case of fragment B, the 76-bp protection (site III) is comparable to that determined with aerobactin at the same molar ratio, in spite of a great difference in the complexation rate (28% versus 78%). Owing to the presence of two binding sites on the fragment A, the histograms (Fig. 3 H_b) were established considering the results from footprinting experiments (shown below). Among 200 analyzed molecules, 22 presented ambiguous sites I and II and were rejected. From the 178 analyzable complexes, 88% have a single binding site occupied (56% on site I and 32% on site II), indicating a higher affinity of Fur for site I. A few molecules (12%) are double-liganded but no loop formation was observed. Fur polymerization

Table I

	ratio	% of fixation	Protection (bp)
Aerobactin	20	58%	34 ± 7
	50	65%	59 ± 13
	80	78%	83 ± 23
	150	95%	89 ± 27
HLY A I	80	50%	41 ± 11
II			45 ± 12
HLY B III	80	28%	76 ± 20

occurs in a much higher extent on hemolysin DNA as compared to aerobactin, especially for fragments B where 28% of the molecules are complexed with a mean protection of 80 bp. Such observations suggest a cooperative phenomenon.

Biochemical studies

When aerobactin DNA was incubated with increasing concentrations of Fur, two retarded bands were detected at 10 and 50 nM Fur (Fig. 4 A), which most likely correspond to complexes with one or two sites occupied respectively by the repressor (17). When the hemolysin fragments A and B were incubated with Fur, a shift occured at 50 nM Fur (Figs. 4 B and 5 A). At higher Fur concentrations (≥ 250 nM Fur), additional bands with slower migration rates appeared as well, suggesting that the protein might bind to additional regions and/or polymerize on DNA fragments (16). A competition with a 30-molar excess of non-labeled A or B fragments diminished the amount of Fur-bound labeled DNA (Figs. 4 C and 5 B, lanes 3 and 7). Similar competition with pBR322 did not change the equilibrium (lanes 4 and 8), thus demonstrating the specificity of the interaction.

Footprinting experiments were then performed with both *hly* fragments, using different Mn^{2+} and Fur concentrations. The pattern of DNase I digestion, obtained with A and B probes, is shown in Figs. 4 and 5 respectively. In the absence of Mn^{2+} (lane 1), no protection was observed, even in the presence of high concentrations of Fur (500 nM). In excess of Mn^{2+} (100 µM), three protected regions were detected and designated as site I (50 bp), site II (≈ 60 bp) for fragment A, and site III (≈ 80 bp) for fragment B. Similar patterns were obtained on complementary strands (not shown). Fur-bound DNA regions are indicated in the 5' non-coding sequence of pANN681 (Fig. 6). As low as 25 µM Mn^{2+} was sufficient to promote the repressor binding.

DISCUSSION

Specific Fur-DNA interactions with the promoter region of aerobactin have been visualized by EM for the first time. The mapping data agree with the existence of two adjacent Fur-binding sites (31 + 19 bp) described by de Lorenzo *et al.* (3), but also reveal an extension of the protection (≈ 85 bp). Interestingly, this particularly large size determined at high protein/DNA ratios (80 or 150), correponds to the protection of the two adjacent promoters P1

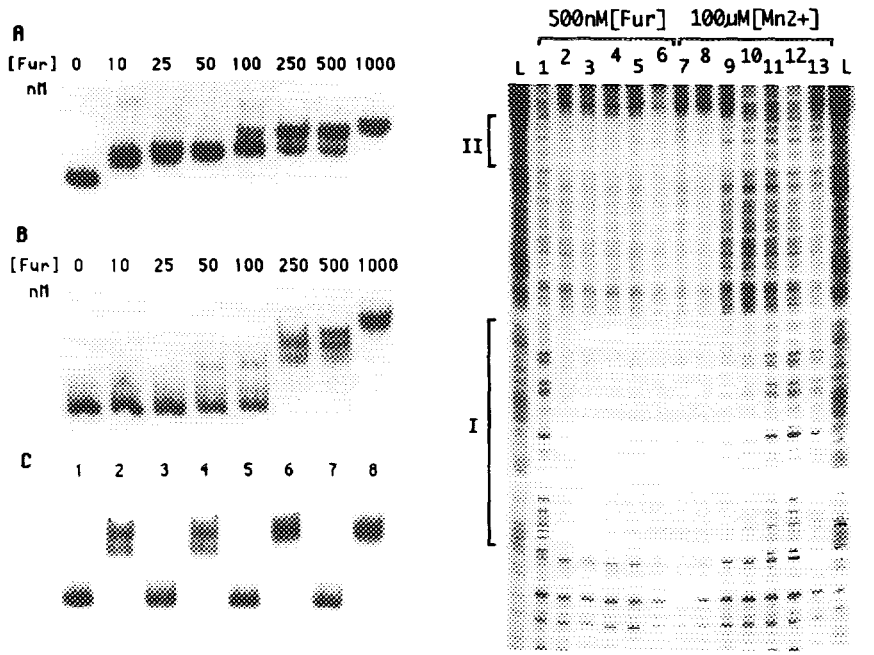

Fig. 4. **Binding of Fur to the promoter region of aerobactin and hemolysin operons.** Gel-retardation assays: (A) The end-labeled 645-bp *Hind*III-*Sal*I fragment (≤ 0.1 nM) carrying the promoter region of the aerobactin operon was incubated with increasing concentrations of Fur in the presence of 100 µM $MnCl_2$, as indicated on top of the figure. (B) The end-labeled 370-bp *hly* fragment A (about 0.1 nM) was incubated with various concentrations of Fur, as indicated.
(C) Competition assays performed with fragment A, using a large excess (30x molar) of either non-labeled fragment A (lanes 3 and 7) or non-labeled pBR322 DNA (lanes 4 and 8). Lanes 1 and 5: no Fur; lanes 2 to 4: 250 nM Fur; lanes 6 to 8: 500 nM Fur.
DNAse I digestion of the *hly* fragment A (coding strand): The 370-bp fragment (0.1-0.5 nM) containing the promoter region was digested with DNase I in the presence of various concentrations of Fur protein and Mn^{2+}. The lanes labeled L are the Maxam & Gilbert C+T sequencing reactions performed on the same fragment. Left lanes (1 to 6), digestions with 500 nM Fur and increasing Mn^{2+} concentrations: lane 1, no Mn^{2+}; lane 2, 25 µM Mn^{2+}; lane 3, 50 µM Mn^{2+}; lane 4, 75 µM Mn^{2+}; lane 5, 100 µM Mn^{2+}; lane 6, 150 µM Mn^{2+}. Right lanes (7 to 13), digestions with 100 µM Mn^{2+} and decreasing concentrations of Fur: lane 7, 1000 nM Fur; lane 8, 500 nM Fur; lane 9, 250 nM Fur; lane 10, 100 nM Fur; lane 11, 50 nM Fur; lane 12, 25 nM Fur; lane 13, no Fur. Protected regions (sites I and II) are indicated.

and P2 (3,4). Such a result reveals the tendency of Fur to polymerize from its target sites as previously proposed (3) and suggests pauses during the polymer elongation. Pause mechanism could be related to the DNA local conformation, since this regulatory region is an unusually AT-rich region flanked by GC-rich sequences, as previously described (4). Polymerization of the protein is more pronounced on hemolysin DNA, since fragments containing large regions covered with Fur were seen among numerous unbound fragments, thus suggesting a cooperative mechanism. The large size of the DNA protections (30 to 80 bp), determined by footprinting in several Fur-regulated systems, is likely to result from the polymerization of Fur onto DNA. This property could indeed fit with the existence of adjacent binding sites, as described for aerobactin (3), enterobactin (7) and Mn-superoxide dismutase (8) gene promoter regions.

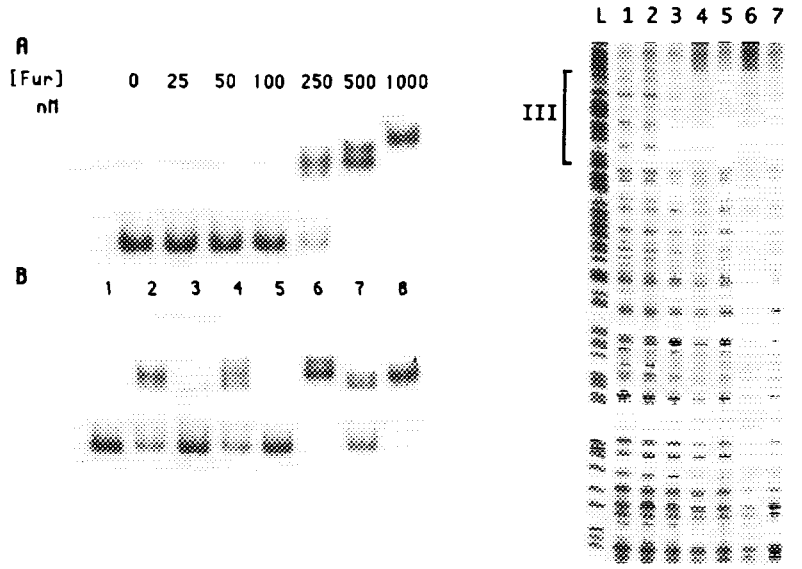

Fig. 5. **Binding of Fur to the *hly* fragment B.** Gel-retardation assay: (A) The end-labeled fragment (about 0.1 nM) was incubated with increasing Fur concentrations, as indicated on top of the figure. (B) Competition assays performed with fragment B, using a 30-molar excess of either non-labeled fragment B (lanes 3 and 7) or non-labeled pBR322 DNA (lanes 4 and 8). Lanes 1 and 5: no Fur; lanes 2 to 4: 250 nM Fur; lanes 6 to 8: 500 nM Fur.
DNase I digestion of the fragment B (non-coding strand): Labeled DNA (0.1-0.5 nM) was digested in the presence of various metal and Fur protein concentrations. Lane L: ladder of sequencing reactions (T tracks of a known sequence) used as size markers to localize the footprinted region. Lane 1, 500 nM Fur, 400 µM 2,2'-dipyridyl, no Mn^{2+}. Lanes 2 to 6, digestions in the presence of 100 µM Mn^{2+} and increasing concentrations of Fur. Lane 2, no Fur; lane 3, 100 nM Fur; lane 4, 250 nM Fur; lane 5, 500 nM Fur; lane 6, 1000 nM Fur. Lane 7, digestion in the presence of 25 µM Mn^{2+} and 500 nM Fur.

Furthermore, EM, gel retardation assays and footprinting experiments allowed to identify three Fur-binding sites within the 5' non-coding region of the *hly* plasmid pANN681. Comparison of these sequences with the consensus "iron box" (3) revealed homologies. Thus, deviation of the Fur-binding sites (3-8) from the consensus sequence could explain the variations in Fur affinities, as those observed between promoter regions of the aerobactin and hemolysin operons in gel retardation assays and EM. In addition, it is worth noting the absence of a palindromic sequence in the *hly* repressor binding sites, indicating that the symmetrical nature of the target DNA regions is not always necessary for their recognition by Fur.

Analysis of DNA-protein interactions requires the use of different methodologies. The combination of gel retardation assays, footprinting experiments and quantitative EM analysis appears to be a convenient approach to obtain original and complementary informations. It is especially appropriate when studying phenomena such as protein polymerization. Although EM is not as resolutive as DNase I footprinting, it provides original information such as different behaviours of the protein within its recognition sites, especially in the case of Fur which tends to polymerize on target DNA. As a bacterial repressor, Fur would be expected to interfere directly with the binding of RNA polymerase to the promoter, but the presence of Fur-binding

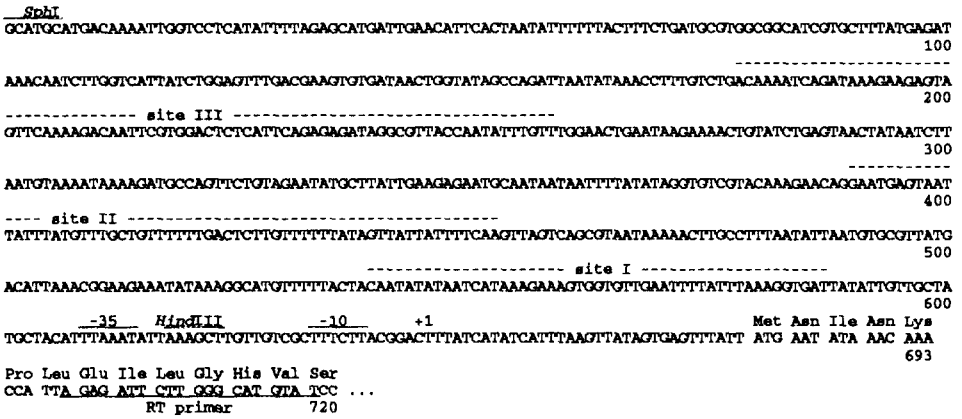

Fig. 6. **Representation of Fur footprints in the pANN681 *hly* regulatory region.** The 1-kb *Sph*I-*Bam*HI region of pANN681 was sequenced from single-stranded DNA templates, by use of the Sequenase 2.0 Kit from United States Biochemical. This sequence has been assigned the Genbank/EMBL accession number L01627.
The transcriptional initiation site (+1) was determined by reverse transcriptase mapping as described (18), using a 20-mer oligonucleotide (RT primer) and total RNA from *E. coli* DH5α(pANN681).
Fur footprints (sites I, II and III) are delineated by hatched lines.

sites upstream from the *hly* pANN681 promoter calls for different hypotheses such as modifications of the DNA conformation and/or topology. The different affinities of Fur for unrelated target sites, as well as the various extents of protein polymerization could be suggested also to understand the variability observed in the levels of repression for different promoters.

ACKNOWLEDGMENTS

We are grateful to M. Barray, A. Barbin, and E. Larquet for their technical assistance and to B. Révet for his contribution in the development of the digitization of the molecules and the computer programs. We are particularly indebted to E. Delain and Lorna Saint-Ange for helpful comments and critical reading of the manuscript.

REFERENCES

1. Bagg, A., and Neilands, J. B. (1987). Microbiol. Rev. 51, 509-518.
2. Braun, V., Schäffer, S., Hantke, K., and Tröger, W. (1990). In: *The Molecular Basis of Bacterial Metabolism*. Colloquium Mosbach 1990. Springer-Verlag Berlin Heidelberg, pp 164-179.
3. de Lorenzo, V., Wee, S., Herrero, M., and Neilands, J. B. (1987). J. Bacteriol. 169, 2624-2630.
4. Bindereif, A., and Neilands, J. B. (1985). J. Bacteriol. 162, 1039-1046.
5. de Lorenzo, V., Herrero, M., Giovannini, F., and Neilands, J. B. (1988). FEBS Eur. J. Biochem. 173, 537-546.
6. Griggs, D., and Konisky, J. (1989). J. Bacteriol. 171, 1048-1054.
7. Brickman, T., Ozenberger, B., and McIntosh, M. (1990). J. Mol. Biol. 212, 669-682.
8. Tardat, B., and Touati, D. (1993). Mol. Microbiol. 9, 53-63.

9. Le Cam, E., Théveny, B., Mignotte, B., Révet, B., and Delain, E. (1991). J. Electron Micr. Tech. 18, 375-386.
10. Grünig, H. M., Rutschi, D., Schoch, C., and Lebek, G. (1987). Zbl. Bakt. Hyg. A 266, 231-238.
11. Lebek, G., and Grünig, H. M. (1985). J. Bacteriol. 50, 682-686.
12. Grünig, H. M., and Lebek, G. (1988). Zbl. Bakt. Hyg. A 267, 485-494.
13. Théveny, B., and Révet, B. (1987). Nucl. Acids Res. 15, 947-958.
14. Dubochet, J., Ducommun, M., Zollinger, M., and Kellenberger, E. (1971). J. Ultrastruct. Res. 35, 147-167.
15. Muzard, G., Théveny, B., and Révet, B. (1990). EMBO J. 9, 1289-1298.
16. de Lorenzo, V., Giovannini, F., Herrero, M., and Neilands, J. B. (1988). J. Mol. Biol. 203, 875-884.
17. Wee, S., Neilands, J. B., and Seetharam, R. (1988). Biol. Metals 1, 62-68.
18. Uzan, M., Favre, R., and Brody, E. (1988). Proc. Nat. Acad. Sci. USA 85, 8895-8899.